

# Holographic Recording on Photopolymers Containing Pyrene for Enhanced Fluorescence Intensity

Hyunjin Oh, Jeonghun Kim, and Eunkyong Kim\*

Department of Chemical and Biomolecular Engineering, Yonsei University, 262 Seongsanno, Seodaemun-gu, Seoul, 120-749, Korea

Received March 28, 2008; Revised Manuscript Received July 27, 2008

**ABSTRACT:** Photopolymer films containing pyrene were studied for fluorescence intensity enhancement by holographic recording. Photopolymer films were prepared from a solution containing a monomer mixture of *s*-triazine dimethacrylic monomer (DT) and ethylene glycol phenyl ether acrylate (PA), polysulfone as a binder, pyrene as a fluorescent dopant, and a visible light sensitive photoinitiator. The films were exposed by means of holographic techniques, resulting in a spatial intensity distribution in the films. The diffraction efficiency of the film containing 1 wt % of pyrene reached a maximum of 93%. The fluorescence intensity of the film was enhanced in conjunction with diffraction efficiency growth, proving that the increase in the fluorescence intensity of the film originated from the increased pyrene monomer emission in response to the increased viscosity around the pyrene molecules. The enhancement of the fluorescence intensity of the recorded area was  $\sim 2$  in reference to the unrecorded area. The recorded area showed grating, which could be identified by transmittance as well as fluorescence scan. The grating spacing and fluorescence intensity of the recorded area were correlated to the pyrene content and incident angle of recording beam.

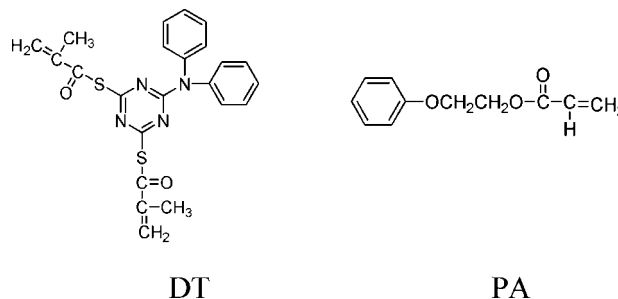
## Introduction

Photopolymer films exploited in holographic storage media have been examined for high density optical data storage<sup>1–5</sup> because of such advantages as their large dynamic range, high light sensitivity, flexibility, and good optical properties over other media such as crystals.<sup>6–10</sup> In photopolymer films, dispersed monomers such as acrylates are polymerized during holographic recording and thus the viscosity of the medium is increased. Specifically, viscosity modulation will be generated along with refractive index modulation as polymerization by the interference light occurs in the constructive interference region.

In this paper we investigate the effect of holographic recording on a fluorescent photopolymer film that may have advantages over traditional photopolymers. The fluorescence of the film offers additional readability while sharing the same characteristics of high diffraction efficiency and parallel readout capability of the holographic recording. In addition, the holographic recording on the fluorescent photopolymer films could provide a unique method to provide a fluorescent pattern on basically any substrates with high fluorescence intensity. The active portion of the medium is a photopolymer that has been used for holographic recording as previously reported.<sup>11–15</sup> To produce fluorescence, the photopolymer is doped with an organic fluorescent dye. Pyrene was chosen as a fluorescent dye because its photophysics is well understood.<sup>16</sup>

It has two excited states, monomer and intermolecular excimer, of which emission intensity is highly dependent on the medium viscosity. Holographic recording occurs during the photopolymerization of monomers which have dimethacrylate (DT)<sup>11</sup> and acrylate units (PA):

Photopolymerization of these monomers can be regarded as a process in which monomer units are immobilized by linking them together in a polymeric network. Therefore, the fluorescence of the photopolymer film containing pyrene is enhanced as recording proceeds since the viscosity of the medium is increased as a result of the polymerization. Herein we report



the effect of pyrene content and recording angle on the fluorescence intensity and grating formation.

## Results and Discussion

**Optical Properties of the Photopolymer Film Containing Pyrene.** The photopolymer film containing pyrene was optically transparent and fluorescent with the pyrene content up to 10 wt %. The fluorescent films were sensitive to visible light, suitable for holographic recording. In our photopolymer system, absorption by the photoinitiator (Irgacure 784) produces a radical. Free radical polymerization of DT and PA is then initiated by the radical.

Figure 1 shows UV–vis spectra and emission spectra for P2 which contained 1 wt % of pyrene (Table 1). The film was yellow-brown before holographic recording due to the absorption at the visible region by the photoinitiator (Irgacure 784). After holographic recording the film was bleached, showing only absorption below 400 nm. The fluorescence emission spectrum of the unrecorded polymer film consisted of a strong band centered at  $\sim 400$  nm and broad, structureless emission centered at  $\sim 530$  nm, which are characteristic of the emission for monomeric pyrene and excimer (excited dimer), respectively. An excimer is known to be formed by the diffusion controlled reaction between a molecule in the excited state and another in the ground state. Interestingly, the fluorescence emission of the film was intensified after holographic recording as shown in Figure 1 (b) and in the photograph in Figure 1 (c). Thus the recorded area appeared as a circle, which is visually recognizable as the recorded area is more emissive than the unrecorded area.

\* Author to whom correspondence should be addressed. E-mail: eunkim@yonsei.ac.kr.

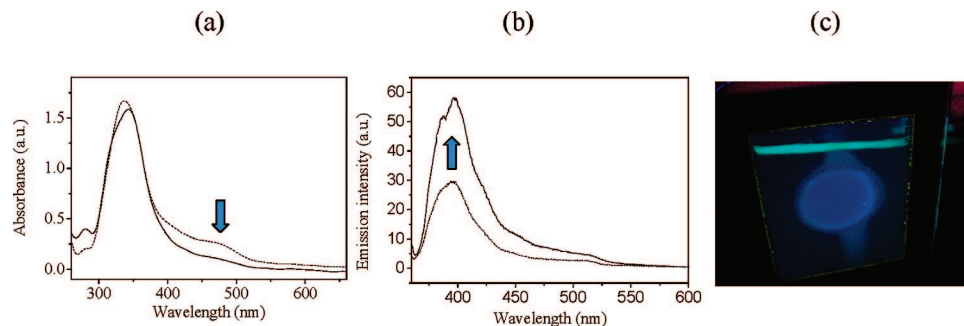


**Figure 1.** (a) UV-vis and (b) fluorescence spectra of the film P2; holographic recorded part (solid line) and unrecorded part (dashed line). (c) A digital photograph for the fluorescence of the recorded film (P2), coated on a plate size of  $5 \times 6 \text{ cm}^2$ , under 365 nm UV lamp.

**Table 1.** Effect of Pyrene Content on the Diffraction Efficiency ( $\eta$ ) and Fluorescence Intensity Ratio ( $R$ )<sup>a</sup>

sample code	pyrene (mmol)	wt % of pyrene <sup>b</sup>	mol fraction of pyrene ([Py]) <sup>c</sup>	thickness (cm) <sup>d</sup>	$\eta$	$\Delta n^e$	sensitivity (cm <sup>2</sup> /mJ), $\times 10^{-5}$	$R$	$\xi^f$
P0	0	0	0	0.0125	0.69	0.0012	4.6		1.00
P1	0.02	0.5	$8.7 \times 10^{-3}$	0.0128	0.79	0.0013	5.6	16.9	1.78
P2	0.03	1	$1.6 \times 10^{-2}$	0.012	0.93	0.0017	13.0	20.3	2.07
P3	0.10	3	$4.7 \times 10^{-2}$	0.0112	0.74	0.0014	2.5	3.8	2.07
P4	0.16	5	$7.7 \times 10^{-2}$	0.011	0.67	0.0013	1.2	1.5	1.23
P5	0.35	10	$1.5 \times 10^{-1}$	0.013	0.60	0.0010	0.64	0.1	0.98

<sup>a</sup> Under the recording beam intensity of  $0.88 \text{ mW/cm}^2$  and incident beam angle of  $30^\circ$ . <sup>b</sup> Weight percentage of pyrene in a mixture of PES, DT, PA, pyrene and photoinitiator. <sup>c</sup> Molar ratio between pyrene and total moles of PES, DT, PA, pyrene, and photoinitiator. <sup>d</sup> The thickness was determined by use of mechanical calipers. <sup>e</sup> Refractive index change between the interference determined from eq 11 using  $\eta$  and thickness of the film. <sup>f</sup> Fluorescence enhancement as a ratio of the fluorescence intensity at 400 nm between the recorded and unrecorded area.

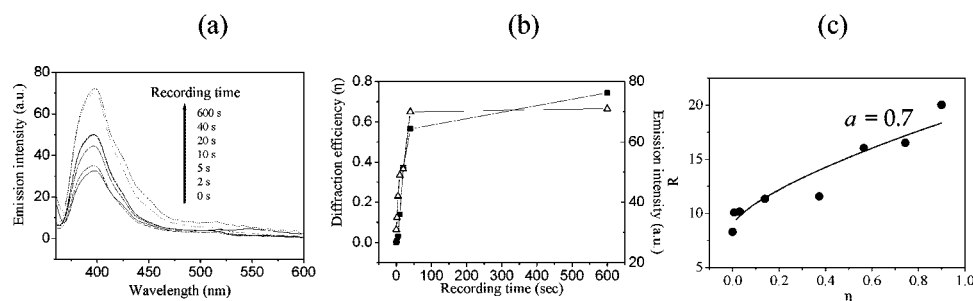


**Figure 2.** (a) Spectral changes in the photopolymer film, P2, upon holographic recording with a 491 nm laser according to recording time. (b) Plot of diffraction efficiency (■) and fluorescence intensity (□) against recording time (s). (c) Correlation of  $R$  against  $\eta$  according to eq 8 with  $a$  value of 0.7.

The ratio of the fluorescence intensity between the recorded and unrecorded areas was 2.07. The fluorescence yield on a polymeric film containing pyrene was determined based on a PMMA film doped with anthracene as a reference.<sup>17</sup> The fluorescence yields were 1.8 and 4.3% for the film unexposed and exposed (recorded) area, respectively.

Such an increase in fluorescence intensity from the film containing the pyrene probe could be originated from the increased monomeric pyrene emission in an increased medium viscosity after holographic recording. During the holographic recording the unsaturated monomers (DT and PT) are polymerized and the microviscosity around pyrene increased as a result of the photo cross-linking reaction of the monomers. It has been well-known that the ratio of monomeric emission (highly fluorescent) to excimer emission (low fluorescent) is a linear function of the medium viscosity.<sup>16</sup> The growth of diffraction efficiency should then match the emission intensity growth. Indeed, Figure 2 (a) shows that the emission intensity of the recorded part is increased and strongly dependent on the diffraction efficiency growth. After diffraction efficiency reached maximum value, there was no more fluorescence intensity increase.

The ratio of the fluorescence intensity for monomers against excimer ( $R = I_M/I_E$ ) is known to be linearly dependent on the medium viscosity<sup>16</sup> and can be written as

$$R = k_1 \rho [\text{Py}]^{-1} \quad (1)$$

where  $\rho$  is the viscosity coefficient,  $[\text{Py}]$  is the concentration of pyrene, and  $k_1$  is a constant. The fluorescence ratio ( $R$ ) is a measure of the microviscosity around the fluorescent probe. During polymerization, the microviscosity increases and the volume decreases. Diffraction efficiency ( $\eta$ ) is determined from the diffracted light intensity ( $I_D$ ) and transmitted light intensity ( $I_T$ ) during holographic recording. There is absorption ( $I_A$ ) of the writing light (491 nm) by the film media, due to the absorption mainly by the photoinitiator. Thus the sum of  $I_D$  and  $I_T$  is always smaller than  $I_0$ . Thus  $I_D$  is related to  $\eta$  according to eq 3:

$$\eta = I_D / (I_D + I_T) = I_D / (I_0 - I_A) \quad (2)$$

$$I_D = (I_0 - I_A) \eta \quad (3)$$

where  $I_0$  is the intensity of the recording beam. From the transmittance spectra obtained from Figure 1 (a), the absorptions

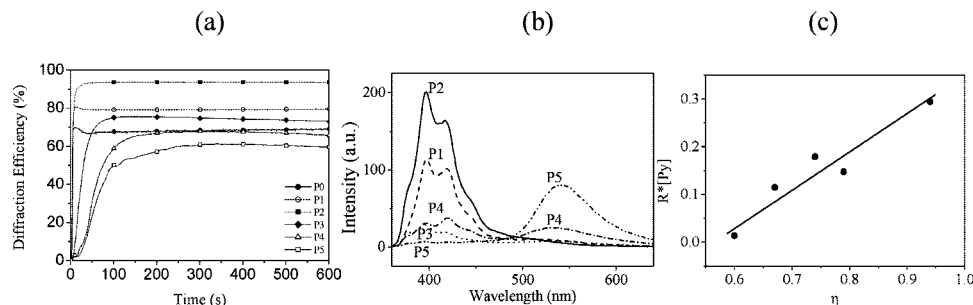


**Figure 3.** (a) Diffraction efficiency of the films containing different pyrene concentrations. (b) Fluorescence spectra for the recorded part of the films containing different pyrene concentrations. (c) Plot of  $R[Py]$  against  $\eta$ .

were 12% and 5% for the films before and after holographic recording, respectively. The relation between intrinsic viscosity ( $\rho$ ) and degree of polymerization ( $z$ ) is represented as  $[\rho] = K(z)^a$  or  $[\rho]_{C=0} = K(M_p)^a$ , by Mark–Houwink–Sakura equation, where  $K$  and  $a$  are constants and  $M_p$  is the viscosity average molecular weight.<sup>18</sup> Different  $a$  values have been reported depending on the structure of monomers and polymers under different reaction media. In this study the viscosity increase of the medium is originated from the polymerization of the monomers upon holographic recording and can be represented as eq 4.

$$\rho(z) = (1 + Kz^a) \cdot \rho_0(z) \quad (4)$$

where  $z$  is the degree of polymerization, and  $\rho(z)$  and  $\rho_0(z)$  are the viscosity of the medium after and before polymerization.

Diffraction of light arises from the refractive index modulation originating from the polymerization of the monomers under the interference light (local) and the polymerization induced by the diffusion of the monomers from the dark region (nonlocal polymerization).<sup>15</sup> Thus the intensity of the diffracted light ( $I_D$ ) is a measure of conversion and related to the extent of polymerizations ( $z$ ) of monomers. To simplify we assume the relationship between  $I_D$  and  $z$  as a linear.

$$I_D = k_2 z \quad (5)$$

$$z = \eta(I_0 - I_A)/k_2 \quad (6)$$

where  $k_2$  is a constant. Then, eq 4 rearranged to a function of viscosity against diffraction efficiency and pyrene content.

$$\rho(z) = \{1 + K(\eta(I_0 - I_A)/k_2)^a\} \cdot \rho_0(z) \quad (7)$$

$$R = k_1(1 + Kk_3^a \eta^a) \rho_0(z) [Py]^{-1} \quad (8)$$

where  $k_3$  is  $((I_0 - I_A)/k_2)^a$ .

Therefore, the relationship between fluorescence intensity ratio ( $R$ ) against diffraction efficiency ( $\eta$ ) and pyrene content can be set up.  $R$  was correlated to  $\eta$ , as shown in Figure 2 (c) when the pyrene content was 1 wt % (molar fraction of 0.016) of the monomer. The experimental data were well matched when  $\alpha$  was 0.7–0.8.<sup>19a</sup> From the correlation of  $R$  against  $\eta$  in eq 8 using 0.7 for  $a$  value, the term  $k_1 \cdot \rho_0(z)$  was determined as 0.14 and  $k_2$  as 22.49/mW (0.74 cm<sup>2</sup>/mW) under the light intensity ( $I_0$ ) of 0.80 mW/cm<sup>2</sup>. When the diffraction efficiency of the film reaches to 100%,  $I_D$  becomes 0.76 mW/cm<sup>2</sup>. Then the degree of polymerization ( $z$ ) could be determined as 1.02, which is close to 1 for complete polymerization, using the  $k_2$  value and  $I_D$ . This result verifies the validity of the relationship between  $R$  and  $\eta$  as in eq 8. Interestingly the simulated  $a$  value of 0.7 corresponds to the Mark–Houwink exponent of  $a$  for PMMA.<sup>19b–d</sup> Therefore eq 8 seems useful for the correlation of  $R$  against  $\eta$  of a photopolymer containing pyrene. It is suggested for other fluorophore<sup>13</sup> that the distributions of fluorophore become more highly concentrated in the polymer-

ized regions during the diffusion of monomers, to enhance the fluorescence grating. However, the relationship in eq 8 indicates that the fluorescence enhancement in this system is mainly attributed to the viscosity change rather than the diffusion of the fluorophore.<sup>13</sup> Detailed studies on diffusion of fluorophores during the holographic recording is in progress using a photo-curable fluorophore to quantify the effect of diffusion.

**Effect of the Pyrene Content on the Diffraction Efficiency of the Films.** The effect of the pyrene content on the diffraction efficiency of the films is dramatic. In the photopolymer without pyrene, the peak diffraction efficiency is typically ~70% under 491 nm laser. Maximum diffraction efficiency ( $\eta_{\max}$ ) of the photopolymer doped with a small amount of pyrene was higher than that of the undoped photopolymer. When the content of pyrene was 1 wt %,  $\eta_{\max}$  reached 93%, but it decreased when the pyrene content was more than 3 wt % as compared in Figure 3 (a). It was also noteworthy that the growth of diffraction efficiency was faster in the photopolymer containing pyrene when the pyrene content was up to 3 wt %. In the photopolymer containing excess pyrene where the content was higher than 5 wt %, the  $\eta_{\max}$  values were decreased and the growth of diffraction efficiency was slower than that without pyrene (P0), possibly due to the hindrance in diffusion of monomers by the excess pyrene molecules in the film.

The sensitivity of the photopolymer films was determined by using the following equation:

$$S = \frac{\Delta n}{I t} \text{ (cm}^2/\text{mJ)} \quad (9)$$

where  $\Delta n$  is refractive index change,  $I$  is the intensity of the laser (0.8 mW/cm<sup>2</sup>), and  $t$  is the exposure time.<sup>20</sup> The sensitivity was higher in the film doped with a small amount of pyrene (P1 and P2) than in the undoped film, as listed in Table 1.

Such increased diffraction efficiency growth and higher sensitivity in photopolymers doped with pyrene suggests that pyrene molecules facilitate the polymerization possibly as a photosensitizer/photoinitiator<sup>21,22</sup> or by energy transfer from a pyrene complex with the radical initiator as reported for the complex of electron-rich polynuclear aromatic compounds with cationic photoinitiators.<sup>23,24</sup>

**Fluorescent Grating Formation.** One of the advantages of fluorophore doping into photopolymer is the additional readability of the pattern using a fluorescence microscope. A gap electrode pattern was inscribed on the photopolymer film of P2 through a holographic recording setup. Figures 4 (a) and 4(b) indicate clearly a mask pattern recorded on the photopolymer film. The recorded (exposed) area was darker when examined by an optical microscope under a white light source due to the polymerization of the unsaturated monomers (DT and PA). It was significant that the recorded area (dark part under an optical microscope) became more fluorescent under UV illumination as shown in Figure 4 (b). The recorded area was more emissive



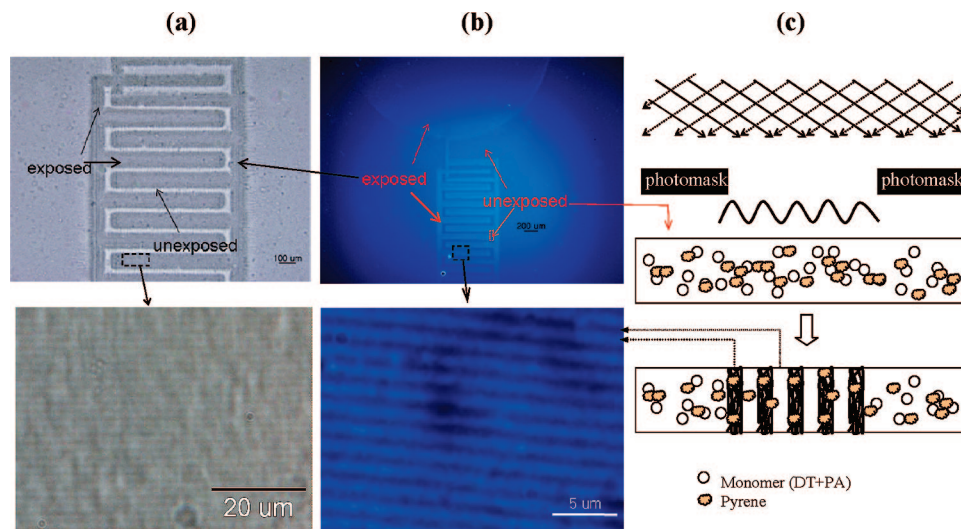


**Figure 4.** (a) Optical microscope image of a gap electrode pattern on P2 inscribed by holographic recording. (b) Fluorescence microscope image of the pattern (film thickness = 120 μm). (c) Scheme of the grating and pattern formation in the photopolymer containing pyrene.

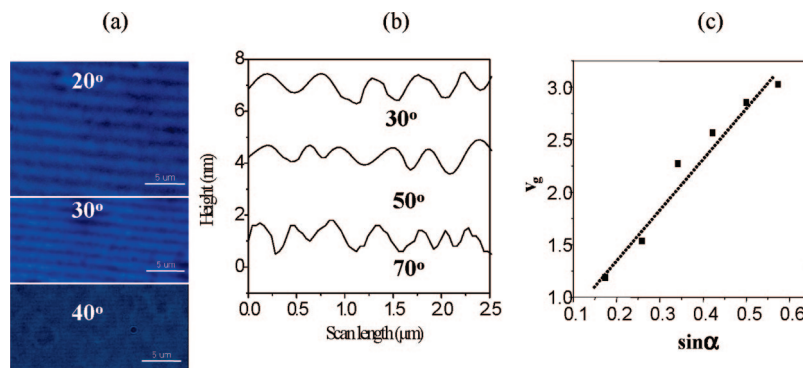


**Figure 5.** (a) Confocal microscopic images of P2 at different recording angle. (b) Grating spacing of P2 after holographic recording determined from a surface profiler. (c) Plot of grating frequency ( $\nu_g$ ) determined from Figure 5 (b) against  $\sin(\alpha)$ .

because of the increased  $I_M/I_E$  due to the increase in viscosity of the polymerized region, as discussed above.

Gratings of black strips were observed in the recorded patterned area under optical transmission microscope when examined using a white light (Figure 4 (a), bottom). These black strips of gratings are photochemically induced by the writing beams in the regions of constructive interference. Regions in the black strips of the radiation interference pattern are now locked by polymerization, and a change of volume and viscosity results to allow the diffusion of molecules to the polymerized regions. Therefore black strips correspond to the more fluorescent strips in the fluorescence confocal microscope under 390 nm excitation (Figure 4 (b), bottom). Figure 4 (c) represents a schematic diagram of the grating and pattern formation in the photopolymer containing pyrene. The mask pattern with a 50 μm gap is inscribed through the photomask (a gap electrode). The grating with a spacing of ~0.65 μm (Figure 4 (b), bottom) is formed by the interference light of the exposed area.

The periodic spacing between the fluorescent gratings corresponds to the interference pattern from the holographic recording. From a surface profiler, the average grating spacing was determined as 0.59 μm. This experimental value agrees with the theoretical value of 0.6 μm<sup>25</sup> from Bragg's law (eq 10), within the range of experimental errors (10%).

$$m\nu_g\lambda = 2n_g \sin \alpha \quad (10)$$

where  $\nu_g$  is the grating frequency (reciprocal of the grating spacing),  $n_g$  is the average refractive index of the grating

medium,  $\alpha$  is the angle of the incidence beam and  $m$  is the order of diffraction, which is equal to 1 in the case of transmission grating.<sup>26</sup>

The grating spacing of the photopolymer determined by a surface profiler at different incident angles was reduced as the angle for holographic recording was increased (Figures 5 (a) and 5 (b)). The frequency ( $\nu_g$ ) was linearly dependent on the sine function of the angle ( $\sin \alpha$ ) according to eq 10 with a slope of 6.695, intercept of 0.05 and correlation factor of 0.986 (Figure 5 (c)). From the slope we could determine the value of the average refractive index of the grating medium ( $n_g$ ) as 1.6438. The bulk refractive index after holographic recording was determined as 1.6149 using a prism coupler at 635 nm.<sup>25</sup> Considering the effect of probing wavelength on the refractive index of media,<sup>27</sup> the  $n_g$  value determined from Figure 5 (c) was matched well to the experimental value.

The fluorescence intensity of the recorded part under different angles was highest when the angle was 30°. This is because the diffraction efficiency is also a function of the angle of the incident beam as shown in eq 11.<sup>28</sup>

$$\eta = \sin^2 \left( \frac{\pi \Delta n d}{\lambda \cos \alpha} \right) \quad (11)$$

Figure 6 (a) shows the diffraction efficiency of the photopolymer film at different incident angles. It was highest when the film was recorded with the incident angle of 30°. As a result the fluorescence intensity was maximized at the angle of 30° but decreased as the angle of the incident beam was larger as

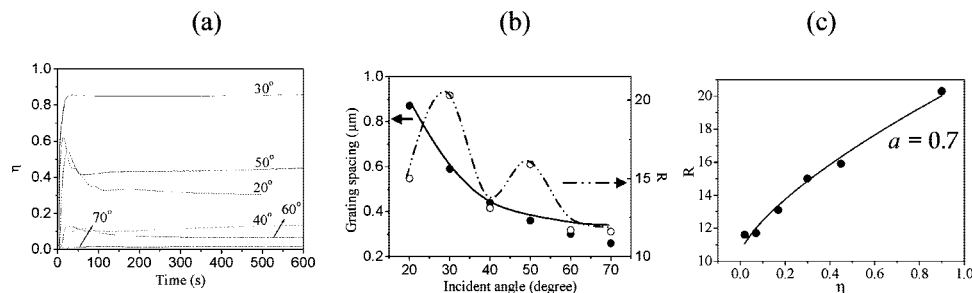


**Figure 6.** (a) The growth of diffraction efficiency for P2 at different incident angles 20–70°. (b) Plot of the grating spacing and  $R$  at different recording angles. (c) Plot of  $R$  against  $\eta$  determined at different incident angles. The solid line corresponds to the correlation of  $R$  against  $\eta$  according to eq 8 with an  $a$  value of 0.7.

compared in Figure 6 (b). The fluorescence intensity ratio for the recorded film of P2 (pyrene mol fraction of 0.016) under different angles was also correlated to the diffraction efficiency, according to eq 8, as shown in Figure 6 (c). Using an  $a$  value of 0.7, we could determine the value of  $k_2$  as  $0.68 \text{ cm}^2/\text{mW}$ .<sup>29</sup> From the  $k_2$  value,  $z$  was determined as 1.08, which is close to 1 at the diffraction efficiency of 100%. This result again strongly backs up the validity of eq 8.

The fluorescence intensity of the photopolymer containing pyrene dopant was well correlated to the diffraction efficiency, which is a function of the viscosity change around pyrene as described above. Therefore holographic recordings on the photopolymer containing pyrene afford a unique method to increase fluorescence intensity, of which intensities are controlled by the recording angle and the content of pyrene. The readout, which is based on the excitation of fluorescence, is nondestructive because the fluorophores in such a solid film do not diffuse easily. This material is nonerasable as the photo cross-linking of the monomer is irreversible in a typical environment. Although there are several reports on fluorescence enhancement from a fluorescent layer on a dielectric grating deposited film as a substrate<sup>30</sup> and references related to detection of polymerization using fluorescent probe, there is no report on the enhancement of fluorescent intensity by holographic recording using photopolymer. Thus this is the first example of fluorescence enhancement in the photopolymer containing pyrene by holographic recording.

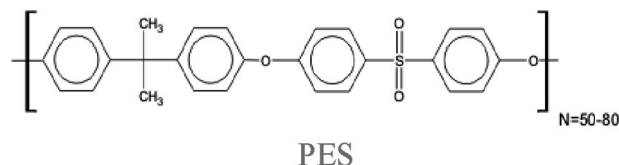
## Conclusion

In conclusion, photopolymer films containing pyrene fluorophore were useful for fluorescence enhancement. The pyrene doped photopolymers showed a higher fluorescence after holographic recording due to the increased monomer/excimer ratio in the polymerized region, where the viscosity around pyrene is high. The fluorescence intensity ratio between the monomer/excimer emission was linearly dependent on the diffraction efficiency. The diffraction efficiency of the photopolymer film containing 1 wt % of pyrene showed a diffraction efficiency reaching 93% within 30 s. However, the photopolymer film containing a larger content of pyrene showed lower diffraction efficiency and lower fluorescence contrast. The use of fluorophores in holographic recording allowed generation of a stable and fluorescent grating pattern. The period of the grating and the intensity of the fluorescence in the recorded area were a function of the angle of the incident beam. The fluorescent intensity reached a maximum when the incident angle was 30°, at which the diffraction efficiency was maximum. The factor of fluorescence enhancement, intensity ratio between the recorded and unrecorded area was 2.07.

## Experimental Section

**Materials.** The triazine dimethacrylate monomer (DT) was synthesized from cyanuric chloride, according to the previously

reported scheme.<sup>11,14</sup> A visible light sensitive mixture consisted of monomers, polysulfone (PES), pyrene, and a visible light sensitive photo initiator.



DT and PA monomers were dissolved in organic solvent and then mixed with polysulfone. The weight ratio of PA:DT:PES: photoinitiator was constant as 30:10:59:1 in all samples. Pyrene was added as a fluorophore with a weight % of 0, 0.5, 1, 3, 5, and 10% to the total weight of PA, DT, PES, and photoinitiator for the samples of P0, P1, P2, P3, P4, and P5, respectively. Therefore the solution for P1, e.g., was prepared by dissolving 0.03 g of pyrene (0.5 wt %), 0.63 g of DT, 1.87 g PA, 3.75 g of polysulfone and 0.05 g of Irgacure 784 in a mixture of 5.07 mL of chloroform and 1.58 mL of TCE. The mixture was stirred and then filtered using membranes of  $0.45 \mu\text{m}$  pore size attached to a Teflon syringe. The solution was coated on glass plate and dried overnight at room temperature and then 40 °C under vacuum.

**Instruments.** UV–vis absorption spectroscopy was performed using a Shimadzu 2550 spectrophotometer and fluorescence was measured with luminescence spectrometer (Perkin-Elmer, model LS55). The optical setup to measure diffraction efficiency of the photopolymer film consisted of a diode laser (491 nm), polarizer, beam splitter and detector, as reported before.<sup>14</sup> The power of the beams was changed by the adjustable PBS, which consists of a rotation half-wave, followed by a polarizing beam-splitter cube and a fixed half-wave plate. The power ratio between the object and reference beam was equal to 1:1 to achieve maximum modulation ratio. The two beams were overlapped on the photopolymer film, and the interference pattern by the two beams was recorded on the film. Diffraction efficiency ( $\eta$ ) was determined from the ratio of  $I_D/(I_T + I_D)$ , where  $I_D$  is the intensity of the diffraction beam (mW) and  $I_T$  is the intensity of the transmission beam (mW). The grating pattern image was examined by optical microscopy (BX-51, Olympus Inc.) and a confocal microscope (LSM 510 META, Carl Zeiss Inc.). The image was obtained using the confocal microscope under 390 nm excitation and collecting the emitted light above 420 nm. The grating spacing and depth after holography recording was determined from a surface profilometer (Tencor Instruments, Alpha-step IQ) with an accuracy of 1 nm. The spacing was determined by averaging the spacing values within the scan length.

**Acknowledgment.** We acknowledge the financial support of the Korea Science and Engineering Foundation (KOSEF) grant funded by the Korea government (MEST) (No. R11-2007-050-01001-0) and Seoul R&BD Program (10816).

## References and Notes

- (1) (a) Dhar, L.; Curtis, K.; Tackitt, M.; Schilling, M.; Campbell, S.; Wilson, W. *Opt. Lett.* **1998**, *23*, 1710. (b) Dhar, L.; Schnoes, G.;

- Wysocki, T. L.; Bair, H.; Schilling, M.; Boyd, C. *Appl. Phys. Lett.* **1998**, *73*, 1337.
- (2) (a) Kim, E.; Park, J.; Cho, S. Y.; Kim, N.; Kim, J. H. *ETRI J.* **2003**, *25*, 253. (b) Park, J.; Kim, E. *Key Eng. Mater.* **2005**, *1039*, 277. (c) Kim, E.; Park, J.; Shin, C.; Kim, N. *Nanotechnology* **2006**, *17*, 2899. (d) Park, J.; Kim, E. *J. Korean Soc. Imaging Sci.* **2002**, *8*, 22.
- (3) (a) Schilling, M. L.; Colvin, V. L.; Dhar, L.; Harris, A. L.; Schilling, F. C.; Katz, H. E.; Wysocki, T.; Hale, A.; Blyler, L. L.; Boyd, C. *Chem. Mater.* **1999**, *11*, 247. (b) Cho, Y. H.; Shin, C. W.; Kim, N.; Kim, B. K.; Kawakami, Y. *Chem. Mater.* **2005**, *17*, 6263. (c) Kim, G. W.; Jun, W. G.; Lee, S. K.; Cho, M. J.; Jin, J.; Choi, D. H. *Macromol. Res.* **2005**, *13*, 477.
- (4) (a) Boyd, J. E.; Trentler, T. J.; Wahi, R. K.; Vega-Cantu, Y. I.; Colvin, V. L. *Appl. Opt.* **2000**, *39*, 2353. (b) Choi, D. H.; Feng, D.; Yoon, H. *Macromol. Res.* **2003**, *11*, 36.
- (5) Waldman, D. A.; Li, H.-Y. *S. Proc. SPIE* **1997**, *3010*, 354.
- (6) Blaya, S.; Carretero, L.; Fimia, A. *Appl. Phys. Lett.* **1998**, *75*, 1628.
- (7) Dhar, L.; Hale, A.; Karz, H. E.; Schilling, M. L.; Schnoes, M. G.; Schilling, F. C. *Opt. Lett.* **1999**, *24*, 487.
- (8) Banyasz, I. *Opt. Commun.* **2000**, *181*, 215.
- (9) Trentler, T. J.; Boyd, J. E.; Colvin, V. L. *Chem. Mater.* **2000**, *12*, 1431.
- (10) Gallego, S.; Ortuno, M.; Neipp, C.; Marquez, A.; Belendez, A.; Tascual, I.; Kelly, J. V.; Sheridan, J. T. *Opt. express* **2005**, *13*, 3543.
- (11) (a) Lee, H.; Sarwade, B. D.; Kim, E. *Opt. Mater.* **2007**, *30*, 637. (b) Oh, H.; Kim, J.; Rameshbabu, K.; Do, J.; Kim, E. *J. Nanosci. Nanotechnol.* **2008**, *8*, 4616.
- (12) Blaya, S.; Acebal, P.; Carretero, L.; Fimia, A. *Opt. Commun.* **2003**, *55*, 228.
- (13) Wang, M. M.; Esener, S. C. *Appl. Opt.* **2000**, *39*, 1826.
- (14) Kim, J.; Sarwade, B. D.; Rameshbabu, K.; Kim, E.; Lee, S. *SPIE Mater. Appl.* **2007**, *6448*, 648806.
- (15) Kim, E.; Choi, K. H.; Rhee, S. B. *Macromolecules* **1998**, *31*, 5726.
- (16) Valdes-Aguilera, O.; Pathak, C. P.; Neckers, D. C. *Macromolecules* **1990**, *23*, 689.
- (17) Guilbault, G. G. *Practical fluorescence: theory, methods, and techniques*; M. Dekker: New York, 1973; pp 1–40.
- (18) (a) Harland, W. G. *Nature* **1952**, *4329*, 667. (b) Ravve, A. *Principles of polymer chemistry*; Plenum Press: New York, 1995; pp 17–23.
- (19) (a) The slope and intercept of the plot were 10.23 and 8.87, respectively. Therefore,  $k_1 \cdot \rho_0(z) \cdot [\text{Py}]^{-1} = 8.87$  (R1),  $Kk_1k_3^a \cdot \rho_0(z) \cdot [\text{Py}]^{-1} = 10.23$  (R2). Thus  $k_1 \cdot \rho_0(z)$  become 0.14 when  $[\text{Py}]$  is 0.016. The ratio of the equation R1/R2 gives  $k_2$  as 0.74. (b) Bischoff, J.; Desreux, V. *Bull. Soc. Chim. Belg.* **1952**, *61*, 10. (c) Mourey, T. H.; Miller, S. M.; Ferrar, W. T.; Molaire, T. R. *Macromolecules* **1989**, *22*, 4286. (d) Hamori, E.; Prusinowski, L. R.; Sparks, P. G.; Hughes, R. E. *J. Phys. Chem.* **1965**, *69*, 1101.
- (20) (a) Murciano, A.; Blaya, S.; Carretero, L.; Ulibarrena, M.; Fimia, A. *Appl. Phys.* **2005**, *B 81*, 167. (b) Tomita, Y.; Nishibiraki, H. *Appl. Phys. Lett.* **2003**, *83*, 410.
- (21) Crivello, J. V.; Jiang, F. *Chem. Mater.* **2002**, *14*, 4858.
- (22) Encinas, M. V.; Majmud, C.; Lissi, E. A.; Scaiano, J. C. *Macromolecules* **1991**, *24*, 2111.
- (23) Crivello, J. V.; Lam, J. H. W. *J. Polym. Sci., Part A: Polym. Chem.* **1979**, *17*, 1059.
- (24) Toba, Y.; Saito, M.; Usui, Y. *Macromolecules* **1999**, *32*, 3209.
- (25) Substituting the refractive index of the photopolymer ( $n_{635} = 1.6149$ ) determined by a prism coupler using a 635 nm laser as a probe beam, the angle of incidence ( $2\alpha = 30^\circ$ ), and the wavelength of the recording beam ( $\lambda = 491$  nm), the grating period was estimated as 0.6  $\mu\text{m}$  from eq 10.
- (26) Barden, S. C.; Arns, J. A.; Colburn, W. S.; Williams, J. B. *PASP* **2000**, *112*, 809.
- (27) Kim, E.; Choi, Y.-K.; Lee, M.-H. *Macromolecules*; **1999**, *32*, 4855.
- (28) Kogelnik, H. *Bell Syst. Tech. J.* **1969**, *48*, 2909.
- (29) The slope and intercept of the plot for  $\alpha = 0.7$  in Figure 6 (c) were 11.26 and 11.13, respectively. Therefore  $k_1 \cdot \rho_0(z) \cdot [\text{Py}]^{-1} = 10.38$  (R3),  $Kk_1k_3^a \cdot \rho_0(z) \cdot [\text{Py}]^{-1} = 10.38$  (R4). The ratio of the equation R3/R4 gives  $k_2$  as 0.68.
- (30) (a) Chance, R. R.; Prock, A.; Silbey, R. *Advances in Chemical Physics*; Prigogine, I., Rice, S. R., Eds.; Wiley: New York, 1978; pp 1–65. (b) Hung, Y.-J.; Smolyaninov, I. I.; Davis, C. C. *Opt. Express* **2006**, *14*, 10825.

MA800691Y